COMMUNICATION

Check for updates

Heparin modulates the cellular uptake of nanomedicines†

Carole Champanhac,[a] Heinrich Haas,[b,c] Katharina Landfester [ID][a] and
Volker Mailänder [ID] *[d,a]

Liposomal formulations are used to improve the safety and cellular absorption of conventional drugs by limiting their interaction with phagocytes. The uptake behaviour of these nanocarriers is affected by the blood composition, and accordingly the presence of an anticoagulant in the blood could have a critical impact on the efficiency of nanomedicines. For the negatively charged liposomes, such as AmBisome®, no significant change in the uptake could be observed when co-incubated with heparin and primary phagocytes. Yet, we observed that a peak of the uptake extent of cationic liposomes was reached at a clinically relevant concentration of heparin for phagocytes and cancer cells. Hence, we recommend avoiding treatment of a heparinized patient with cationic nanomedicines because unexpectedly high uptake can occur in phagocytes.

Introduction

The surface charge (positive or negative) of a nanocarrier (NC) plays a major role in directing its interaction with its surroundings and in defining its cellular uptake efficiency.[1–3] A change in the environment by the addition of a systemic drug, such as the negatively charged heparin, could be expected to change the cellular uptake of NCs. Therefore, patients under dual treatment of heparin combined with a drug nanocarrier could suffer from a decrease in the therapeutic effect of the nanomedicine compared to a patient receiving only the nanomedicine.

[a] Max-Planck-Institute for Polymer Research, Ackermannweg 10, 55122 Mainz, Germany. E-mail: mailaend@mpip-mainz.mpg.de

[b] TRON gGmbH – Translationale Onkologie an der Universitätsmedizin der Johannes, Germany

[c] BioNTech SE, Mainz, Germany

[d] Department of Dermatology, University Medical Center of the Johannes Gutenberg-University Mainz, Langenbeckstraße 1, 55131 Mainz, Germany

†Electronic supplementary information (ESI) available: Detailed methods and supporting figures. See DOI: 10.1039/d0bm01946a

The assessment of the potential of heparin to interfere with the efficiency of nanomedicines is crucial since heparin is the most common anticoagulant used in the clinic.[4] It is given to patients at risk of thrombosis to prevent the activation of the coagulation cascade.[5] Several variants of heparin are available on the market, yet they all share one key property, namely a high negative charge.[6] This glycosaminoglycan is heavily sulfonated, making it one of the naturally most negatively charged molecules.[5,6] To be efficient, heparin is injected intravenously at a concentration of 1.0 IU mL^{-1}, so it will easily get in contact with NCs. We demonstrated that the presence of heparin in plasma affects the cellular uptake of a polystyrene NC, in terms of both extent and target cells.[7,8] This discovery raises concern with liposomal nanomedicines such as AmBisome® which is usually given, after surgery, to patients who are treated with heparin.

A liposome is a closed bilayer phospholipid membrane that is often composed of cholesterol, for stability,[9] and one or several phospholipids, which control the liposome overall charge. FDA-approved liposomes such as Doxil®, used for the treatment of cancer,[10] and AmBisome®, used for the treatment of fungal infections,[11] are electrostatically neutral or negatively charged. Alternatively, gene therapy is attracting attention by promoting the development of positively charged liposomes, as RNA strands adsorb easily on these liposomes by electrostatic interaction.[12] The addition of PEG chains improve the liposomes' stealth[13,14] by minimizing the formation of a biomolecular corona on their surface, which transforms their original synthetic identity into a biological one and plays a crucial role in the cellular uptake of NCs. This acquired identity is defined by the composition of the blood environment.[15,16] The presence of an anticoagulant would modify it, leading potentially to the modulation of uptake of NCs by the target cells and phagocytes.

A major cause of poor therapeutic outcome is the presence of phagocytes, which are specialized in removing nanocarriers from the blood vessels.[17–19] In the case of dual treatment, phagocytes would be the first to be impacted by the new NC

identity, causing modulation in NC's distribution in the organism. To assess the extent of this modulation, we incubated the positively and negatively charged NCs (liposomes and polystyrene) with cells in a medium containing 10% human serum and a range of heparin concentration. The uptake was investigated in a cancer cell model: HeLa cells, a macrophage model: RAW264.7, and two human phagocytes: monocytes and macrophages. We found that for primary phagocytes the presence of heparin heavily modified the uptake of the positively charged nanocarriers, while no significant modulation was observed for the negatively charged NCs.

Materials and methods

All buffers and culture media, unless otherwise specified, were purchased from Sigma-Aldrich, USA.

F5 liposomes (BioNTech, Germany) are composed of DOTMA : cholesterol in a 1 : 1 ratio. AmBisome® liposomes (Gilead Sciences, USA) are composed of HSPC : DSPG : cholesterol in a 4 : 1 : 1.6 ratio. F5 and AmBisome® were labelled with DiO- or DiD-Vybrant dye (Thermo Fisher Scientific, USA) for the cellular uptake experiment. The liposomes were incubated with the dye (250 : 1, v/v) for 30 minutes at 30 °C. The liposomes were then dialysed against water overnight to remove any free dye. Polystyrene nanocarriers (PS NCs) were synthesized by free-radical miniemulsion polymerization. More details on the surfactant and co-monomer used for the nanocarrier synthesis can be found in the ESI.†

The nanocarriers were characterized in terms of surface charge using a Zetasizer Nano Z instrument (Malvern, Germany), size using a Zetasizer S90 instrument (Malvern, Germany), and fluorescence intensity using an Infinity M1000 plate reader (Tecan, USA).

HeLa (human cervix adenocarcinoma (CCL-2)) cells were purchased from American Type Culture Collection (ATCC, USA) and maintained in Eagle's Minimum Essential Medium (EMEM). RAW 264.7 (murine macrophage (TIB-71)) cells were purchased from ATCC and maintained in Dulbecco's Modified Eagle's Medium (DMEM). All media were supplemented with foetal bovine serum (10% v/v, Gibco, USA) and penicillin–streptomycin (100 U mL^{-1}, Gibco). All cells were cultured at 37 °C under a 5% CO_2 atmosphere. To prevent mutation of the cells, passaging was kept under 25. Primary monocytes and macrophages were isolated by the gradient density layer method and cultured in RPMI-1640 media supplemented with 2% (v/v) human serum for respectively 18 h and 7 days, as previously described.[7] The staining procedure can be found in the ESI.†

For the cellular uptake experiments, 10^5 cells were seeded into 24 well plates one day prior to the experiment. Just before the experiment, the culture medium was removed and the cells were washed twice with Dulbecco's Phosphate Buffer Saline (DPBS). Solutions containing 10% human serum and Na-Heparin (Rotexmedica) in DMEM were prepared (more

details can be found in the ESI†) and 30 μg mL^{-1} labelled liposomes or 40 μg mL^{-1} PS nanocarriers were added to the solution. Next, 1.0 mL of nanocarrier solution was added to the cells and incubated for 3 h at 37 °C in the dark. Afterwards, the supernatant was removed, and the cells were washed three times with DPBS, recovered with 0.25% trypsin, and then suspended in DPBS. Twenty thousand events were recorded on a ML CyFlow (Partec, Germany) using two channels: FL1 (exc: 488 nm/em: 527 nm) and FL6 (exc: 640 nm/em: 675 nm).

For the verification of the internalization of the NCs, the cells were incubated with a solution containing 10% human serum, heparin, and 20 μg mL^{-1} nanocarriers for 3 h at 37 °C. In the case of the liposomes, FITC-labelled heparin was used. The supernatant was removed and the cells were washed three times with DPBS. For visualization of the cell membrane, Cell Mask Orange (1 : 1000 dilution) was applied. The images were acquired using a TCS SP5 microscope (Leica, Germany) and three channels were set up: green for the detection of FITC-heparin or the PS NCs (exc: 488 nm/em: 510–540 nm), orange for cell staining (exc: 561 nm/em: 575–590 nm), and red for the liposomes (exc: 633 nm /em: 660–680 nm).

The flow cytometry data analysis was performed using FCS Express V4 and Origin 9.1. GraphPad Prism 8 was used for statistical analysis. In addition, the estimation of the heparin amount per nanocarrier, based on the CLSM images, was performed using PyCharm/OpenCV and LAS X software, and the analysis details can be found in the ESI.†

Results and discussion

Since the liposomes were not fluorescent, we labelled them with DiO- or DiD-Vybrant dyes, which intercalate easily in the liposome membrane. In order to ensure the quality of the labelled liposomes, they were prepared freshly before each cellular uptake experiment. The hydrodynamic diameter, surface charge and fluorescence intensity were measured for each batch. After labelling, the F5 liposomes remained positively charged (+44 mV) and the diameter (166 nm) did not change significantly. Similarly, AmBisome® remained negatively charged (−34 mV) and the diameter remained stable at 108 nm (Table 1). Overall, the labelling step did not change

Table 1 Overview of the physical characteristics of the nanocarriers. Diameter, ζ-potential, and fluorescence intensity are reported as mean ± (standard deviation) of a triplicate measurement

Sample	Diameter (nm)	PdI (a.u.)	ζ-Potential (mV)	Fluo. int. (a.u.)
F5 liposome	166 (4.0)	0.062	+44 (2.5)	n.a.
DiO-F5	167 (2.9)	0.053	+42 (4.1)	1120 (115)
AmBisome	109 (1.6)	0.162	−44 (4.2)	n.a.
DiD-AmB	108 (1.7)	0.136	−34 (7.6)	1560 (95)
PS-SDS-COOH	113 (1.8)	0.090	−56 (1.3)	2895 (120)
PS-Lut-NH$_2$	170 (2.8)	0.335	+2.4 (0.4)	2120 (115)
PS-CTMA-NH$_2$	110 (0.6)	0.084	+42 (0.8)	2175 (150)

significantly the physical characteristics of the liposomes used.

Next, we quantified the cellular uptake extent of the liposomes and polystyrene NCs in the presence of heparin in a physiological medium composed of 10% human serum. We investigated using a range of heparin concentrations centred on the clinical concentration of 1.0 IU mL^{-1}. We chose HeLa cells as a cancer cell model. In the presence of up to 1.0 IU mL^{-1} heparin, we observed a sharp increase of the interaction of F5 liposomes with these cells, as shown by a doubling of the median fluorescence intensity (MFI) between the no heparin (775 au) and 1.0 IU mL^{-1} heparin (1540 au) conditions. However, above 1.0 IU mL^{-1}, all interactions were lost and no liposomal signal could be detected anymore (Fig. 1A). This result was confirmed by confocal laser scanning microscopy (CLSM) (Fig. 1B). We observed that in the absence of heparin, the F5 liposomes were located inside the cells. In the presence of 1.0 IU mL^{-1} heparin, a stronger signal was observed, yet the liposomes were located at the membrane interface. In addition, a clear overlap of the FITC-heparin signal with the liposomes was observed, proving the interaction between heparin and the cationic liposomes (Fig. S1†). AmBisome® liposomes showed a different response to heparin and we observed in its presence a significant decrease of the

MFI from 203 au to 45 au (Fig. 1A). This trend was confirmed by CLSM, which showed that heparin did not interact with AmBisome® as strongly as with F5 liposomes (Fig. 1B, Fig. S2†). Furthermore, we investigated the impact of heparin on the positively and negatively charged PS NCs, and we observed that only the positively charged NCs (PS-CTMA-NH$_2$) were impacted by the presence of heparin. No change in the uptake extent was observed for the negatively charged (PS-SDS-COOH) and stealth (PS-Lut-NH$_2$) nanocarriers (Fig. S3A and S4†).

Next, we used RAW 264.7 cells as a model for macrophages. We found that both liposomes behaved in the same way in the presence of heparin, namely the uptake extent increased (Fig. 1C). The F5 liposomes showed a dose dependent response with a significant increase in the uptake at concentrations above 0.5 IU mL^{-1}. AmBisome® has already been shown to be taken up to a large extent at low heparin concentration leading to apparent saturation at 0.5 IU mL^{-1}. By confocal imaging, we confirmed the internalization of the liposomes by the macrophages (Fig. 1D). Furthermore, the interaction between the liposomes and the cells was also confirmed by imaging (Fig. S5 and S6†). Among the negatively charged (PS-SDS-COOH), stealth (PS-Lut-NH$_2$), and the positively charged (PS-CTMA-NH$_2$) NCs, we observed that only the positively charged NCs were impacted by the presence of heparin, characterized by an increase in the internalization extent (Fig. S3B and S7†).

Finally, we incubated the liposomes with primary phagocytes; we chose monocytes and macrophages as they are the first cells liposomes have to evade when injected intravenously. In the presence of heparin and AmBisome®, no change in the cellular uptake extent was observed for primary monocytes (Fig. 2A) and macrophages (Fig. 2B). The F5 liposomes, on the other hand, were being internalized to a different extent in the presence of heparin. For primary monocytes (Fig. 2A), an inflexion point was observed with the MFI increasing from 525 au to 675 au at 0.5 IU mL^{-1} before dropping to 300 au at 1.0 IU
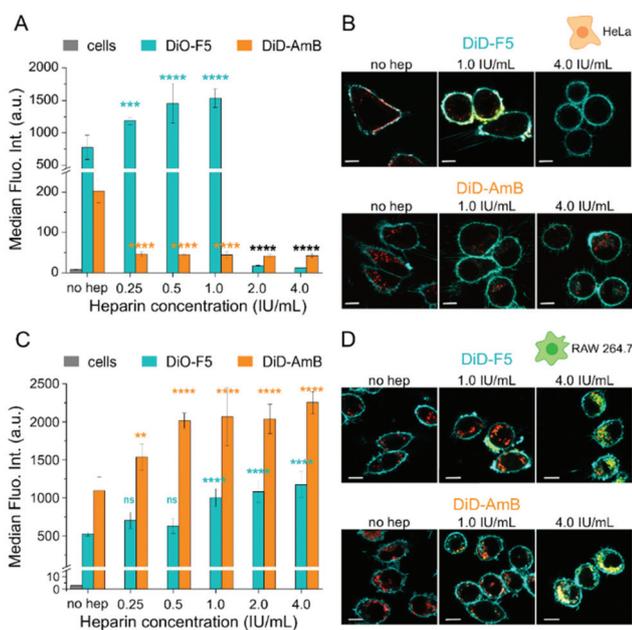

Fig. 1 Cellular uptake of liposomes by (A and B) HeLa cells and (C and D) RAW 264.7 cells after 3 h of incubation at 37 °C with 30 μg mL^{-1} liposomes. (A and C) The median fluorescence intensity was measured at different heparin concentrations. The error bars represent the standard deviation of the average median fluorescence intensity (n = 6). P-Values were calculated using "no hep" condition as the reference; p-values <0.002 are represented with **, p-values <0.0002 with ***, and p-values <0.0001 with ****. (B and D) Internalization and co-localization of the heparin and liposome signal were assessed. The cell membrane is represented in blue, the FITC–heparin in green and liposomes in red. The scale bar represents 10 μm.
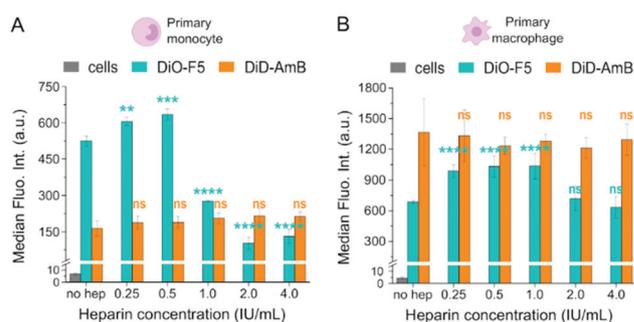

Fig. 2 Cellular uptake of liposomes by (A) primary monocytes and (B) primary macrophages in the presence of heparin after 3 h of incubation at 37 °C. The error bars represent the standard deviation of the mean median fluorescence intensity (n = 6). P-Values were calculated using "no hep" condition as the reference; p-values <0.002 are represented with **, p-values <0.0002 with ***, p-values <0.0001 with ****, and p-values >0.03 are considered non-significant (ns).

mL^{-1}. Primary macrophages have a higher inflexion point, with an increase of the uptake up to 1.0 IU mL^{-1}, as shown by an increase of the MFI from 690 au to 1040 au, before returning to the untreated level starting from 2.0 IU mL^{-1} (Fig. 2B). We also tested the polystyrene nanocarriers in primary phagocytes. We observed that only the positively charged PS NCs (PS-CTMA-NH$_2$) were affected by the presence of heparin when internalized by primary monocytes. For primary macrophages, no change was observed (Fig. S8†).

To understand the uptake pattern observed, we looked at the surface charge of both liposomes, since it is the main variable between them. We ruled out a change in the protein corona composition using the polystyrene nanocarriers. We found a change in the composition of the corona depending on the surface functionalization of the NC and surfactants but no significant change was observed between 1.0 IU mL^{-1} heparin and no heparin conditions (Fig. S9†). Therefore, we focused our attention on the adsorption of heparin on the liposome surface. F5 liposomes are highly positively charged while AmBisome® liposomes are negatively charged, therefore we expected the electrostatic interaction of negatively charged heparin with F5 liposomes to be stronger than that of AmBisome®. To confirm this reasoning, we analysed the images obtained by CLSM. Spots presenting the co-localization of liposomes (red pixels) and FITC-heparin (green pixels) were used to estimate the amount of heparin adsorbed on the liposomes. Indeed, only the heparin molecules strongly adsorbed onto the surface could be internalized alongside the liposomes. Briefly, we extracted the pixels that were green and red (co-localization condition) and we tallied the total intensity of these pixels for the green (heparin) and red (liposomes) channels. The ratio of the intensities corresponds to the amount of heparin per liposome. By this method, we could confirm the higher amount of heparin on positive liposomes. The ratio tends to increase in a concentration dependent manner for the F5 liposomes. Saturation of the F5 liposomes appears to have been reached above 1.0 IU mL^{-1} (Fig. 3 and S10†). This trend was confirmed in both HeLa and RAW 264.7 cells, proving the robustness of the method. On the other hand, no significant change in the ratio was observed for AmBisome®. This analysis confirms the importance of the surface charge for the adsorption of heparin on a nanocarrier.

With the increase in the concentration, the packing of heparin molecules on the surface of the positively charged nanocarriers becomes denser, which should change the apparent surface charge.[7] This could explain the inflexion point of the cellular uptake observed for HeLa cells and primary monocytes (Fig. 3), as the positively and negatively charged NCs are internalized by different mechanisms.[20] On the other hand, macrophages display heparin receptors.[21] Therefore, the uptake of the coated NC could be maintained or even increased due to the specific uptake of the nanocarrier through these receptors.[22]

In our system, free heparin is present in solution alongside serum proteins and nanocarriers. Hence, we expect to have a dynamic evolution of the biomolecular corona over time with a
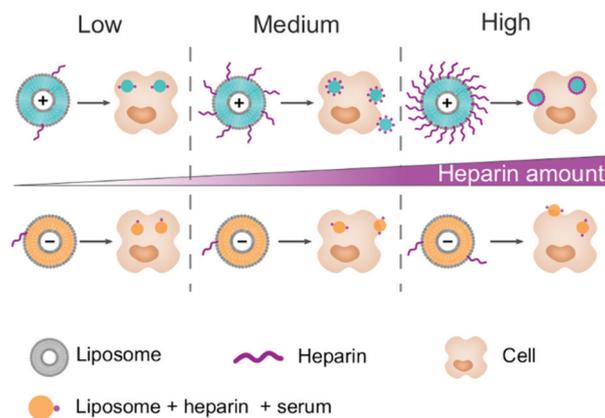

Fig. 3 Schematic representation of the heparin adsorption on liposomes depending on their surface charge and their cellular uptake fate. Light blue liposomes are positively charged (F5) and orange liposomes are negatively charged (AmBisome®). The number of heparin chains (in purple) was estimated at different concentrations of heparin. The number of blue/orange dots in the cell represents on average the uptake behaviour of HeLa, primary monocytes and macrophages. The dots located at the edge of the cell can be either in or out depending on the cell type.

competition between the heparin and serum molecules for their adsorption on the surface of the NCs. Furthermore, in a living organism, heparin will be degraded overtime while the protein concentration should remain stable, and thus the nanocarriers internalized in the first minutes of circulation would be different from the ones internalized several hours later. This leads to a potentially strong fluctuation in the identity of the NCs over time, resulting in an even stronger variation in the cellular uptake extent as we observed with the tested range of concentration.

Conclusions

In short, we have shown that multiple drugs can interact with one another leading to a change in the extent of their uptake by the cells they encounter. In this study, we focused on heparin interacting with liposomes, which is a likely occurrence in hospitals. We observed an inflexion point with a peak of uptake being reached between 0.5 and 1.0 IU mL^{-1} for cationic liposomes. The negatively charged liposomes were also affected with a sharp decrease in the cellular uptake by cancer cells, but no effect was observed for the primary phagocytes. In a clinical environment, it would be better to allow sufficient time to elapse between intravenous unfractionated heparin injection and cationic nanomedicine treatment. This delayed treatment might not be enough for long-lived low molecular weight heparin and fluctuation of the uptake of the nanomedicine can be expected. Indeed, we showed that below the initially injected heparin blood concentration (1.0 IU mL^{-1}), primary phagocytes internalize more NCs than in the absence of heparin, which leads to a decrease in the nanomedicine available for the target cells.

Conflicts of interest

There are no conflicts to declare.

Acknowledgements

References

1 D. Hühn, K. Kantner, C. Geidel, S. Brandholt, I. De Cock, S. J. H. Soenen, P. Rivera-Gil, J.-M. Montenegro, K. Braeckmans, K. Müllen, G. U. Nienhaus, M. Klapper and W. J. Parak, *ACS Nano*, 2013, **7**(4), 3253–3263.

2 C. C. Fleischer and C. K. Payne, *J. Phys. Chem. B*, 2012, **116**, 8901–8907.

3 S. Metwally and U. Stachewicz, *Mater. Sci. Eng., C*, 2019, **104**, 109883.

4 E. I. Oduah, R. J. Lindhardt and S. T. Sharfstein, *Pharmaceuticals*, 2016, **9**(3), 38–50.

5 I. Capila and R. J. Lindhardt, *Angew. Chem., Int. Ed.*, 2002, **41**, 390–412.

6 M. A. Smythe, J. Priziola, P. P. Dobesh, D. Wirth, A. Cuker and A. K. Wittowsky, *J. Thromb. Thrombolysis*, 2016, **41**, 165–186.

7 C. Champanhac, J. Simon, K. Landfester and V. Mailänder, *Biomacromolecules*, 2019, **20**, 3724–3732.

8 S. Schöttler, K. Klein, K. Landfester and V. Mailänder, *Nanoscale*, 2016, **8**, 5526–5536.

9 M.-L. Briuglia, C. Rotella, A. McFarlane and D. A. Lamprou, *Drug Delivery Transl. Res.*, 2015, **5**, 231–242.

10 A. Gabizon, H. Schmeeda and Y. Barenholz, *Clin. Pharmacokinet.*, 2003, **42**(5), 419–436.

11 R. Chopra, S. Blair, J. Strang, P. Cervi, K. G. Patterson and A. H. Goldstone, *J. Antimicrob. Chemother.*, 1991, **28**, 93–104.

12 S. Semple, A. Akinc, J. Chen, *et al.*, *Nat. Biotechnol.*, 2010, **28**, 172–178.

13 D. D. Lasic and D. Needham, *Chem. Rev.*, 1995, **95**, 2601–2628.

14 M. L. Immordino, F. Dosio and L. Cattel, *Int. J. Nanomed.*, 2006, **1**(3), 297–315.

15 C. D. Walkey and W. C. W. Chan, *Chem. Soc. Rev.*, 2012, **41**, 2780–2799.

16 G. Caracciolo, *Nanomedicine*, 2015, **11**, 543–557.

17 T. M. Allen and P. R. Cullis, *Adv. Drug Delivery Rev.*, 2013, **65**, 36–48.

18 E. K.-H. Chow and D. Ho, *Sci. Transl. Med.*, 2013, **5**, 216rv4.

19 C. Corbo, R. Molinaro, F. Taraballi, N. E. Toledano Furman, M. B. Sherman, A. Parodi, F. Salvatore and E. Tascotti, *Int. J. Nanomed.*, 2016, **11**, 3049–3063.

20 E. Fröhlich, *Int. J. Nanomed.*, 2012, **7**, 5577–5591.

21 I. Bleiberg, I. MacGregor and M. Aronson, *Thromb. Res.*, 1983, **29**, 53–61.

22 F. Zhao, Y. Zhao, Y. Liu, X. Chang, C. Chen and Y. Zhao, *Small*, 2011, **7**, 1322–1337.